

# Bose-Einstein condensation and superfluidity of magnetoexcitons in bilayer graphene

Oleg L. Berman,<sup>1</sup> Yurii E. Lozovik,<sup>2</sup> and Godfrey Gumbs<sup>3</sup>

<sup>1</sup>*Physics Department, New York City College of Technology of the City University of New York,  
300 Jay Street, Brooklyn, New York 11201, USA*

<sup>2</sup>*Institute of Spectroscopy, Russian Academy of Sciences, Troitsk, 142190 Moscow Region, Russia*

<sup>3</sup>*Department of Physics and Astronomy, Hunter College of the City University of New York,  
695 Park Avenue, New York, New York 10021, USA*

(Received 30 December 2007; published 21 April 2008)

We propose experiments to observe Bose-Einstein condensation and superfluidity of quasi-two-dimensional spatially indirect magnetoexcitons in two-layer graphene. The energy spectrum of collective excitations, the sound spectrum, and the effective magnetic mass of magnetoexcitons are presented in the strong magnetic field regime. The superfluid density  $n_S$  and the temperature of the Kosterlitz-Thouless phase transition  $T_c$  are shown to be increasing functions of the excitonic density  $n$  but decreasing functions of  $B$  and the interlayer separation  $D$ .

DOI: [10.1103/PhysRevB.77.155433](https://doi.org/10.1103/PhysRevB.77.155433)

PACS number(s): 71.35.Ji, 03.75.Hh, 71.35.Lk, 73.20.Mf

## I. INTRODUCTION

Indirect exciton in coupled quantum wells (CQWs) in the presence or absence of a magnetic field  $B$  have been the subject of recent experimental investigations.<sup>1-4</sup> These systems are of particular interest because of the possibility of Bose-Einstein condensation (BEC) and the superfluidity of indirect exciton formed from electron-hole ( $e$ - $h$ ) pairs. These may result in persistent electrical currents in each quantum well (QW) or coherent optical properties and Josephson junction phenomena.<sup>5-12</sup> In high magnetic fields, two-dimensional (2D) exciton survive in a substantially wider temperature range, as the exciton binding energies increase with magnetic field.<sup>13-19</sup>

In this paper, we consider physical realizations of 2D magnetoexcitonic BEC and superfluidity in two spatially separated graphene layers in high magnetic field (Fig. 1). Recent technological advances have allowed the production of graphene, which is a 2D honeycomb lattice of carbon atoms that form the basic planar structure in graphite.<sup>20,21</sup> Graphene has been attracting a great deal of experimental and theoretical attention because of unusual properties in its band structure.<sup>22-28</sup> It is a gapless semiconductor with massless electrons and holes, which have been described as Dirac fermions.<sup>23</sup> Since there is no gap between the conduction and valence bands in graphene without magnetic field, the screening effects result in the absence of exciton in graphene in the absence of magnetic field. A strong magnetic field produces a gap since the energy spectrum becomes discrete formed by Landau levels. The gap reduces screening and leads to the formation of magnetoexcitons.

We consider two parallel graphene layers separated by an insulating slab (e.g.,  $\text{SiO}_2$ ). The equilibrium system of local pairs of spatially separated electrons and holes can be created by varying the chemical potential by using a bias voltage between two graphene layers or between two gates located near the corresponding graphene sheets (case 1) (for simplicity, we also call these equilibrium local  $e$ - $h$  pairs as indirect magnetoexcitons). In case 1, a magnetoexciton is formed by an electron on the Landau level 1 and hole on the Landau

level  $-1$ . Magnetoexcitons with spatially separated electrons and holes can be created also by laser pumping (far infrared in graphene) (case 2) and by applying perpendicular electric field as for CQWs.<sup>1-3</sup> In case 2, a magnetoexciton is formed by an electron on the Landau level 1 and hole on the Landau level 0. We assume the system is in quasiequilibrium state. Below, we assume the low-density regime for magnetoexcitons, i.e., magnetoexciton radius  $a < n^{-1/2}$ , where  $n$  is the 2D magnetoexciton density.

The paper is organized in the following way. In Sec. II, we represent the eigenfunctions and eigenvalues of the Dirac Hamiltonian for an isolated electron-hole pair without the Coulomb interaction. In Sec. III, the spectrum of isolated indirect magnetoexciton with the spatially separated electron and hole in bilayer graphene is derived applying the perturbation theory respect to Coulomb electron-hole attraction. In Sec. IV, the sound spectrum of collective excitations in weakly interacting gas of magnetoexcitons with dipole-dipole repulsion in bilayer graphene is calculated in the ladder approximation. In Sec. V, the phase transition in the superfluid liquid of magnetoexcitons is analyzed in bilayer graphene. In Sec. VI, we discuss our results.

## II. ISOLATED ELECTRON-HOLE PAIR WITHOUT THE COULOMB INTERACTION

We consider two parallel graphene layers separated by an insulating slab of  $\text{SiO}_2$ . The spatial separation of electrons and holes in different graphene layers can be achieved by

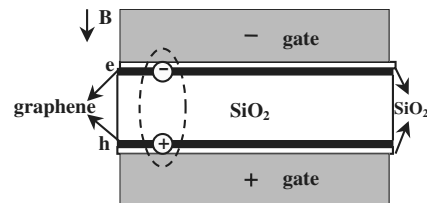


FIG. 1. The indirect magnetoexciton in bilayer graphene in perpendicular magnetic field  $\mathbf{B}$ .

applying an external electric field. Furthermore, the spatially separated electrons and holes can be created by varying the chemical potential by using a bias voltage between two graphene layers or between two gates located near the corresponding graphene sheets. Indirect magnetoexcitons are bound states of spatially separated electrons and holes in an external magnetic field. The ratio of the external voltage  $V_{ext}$  to the interlayer separation  $D$  required to create spatially separated electrons and holes in graphene layers with the 2D density  $n=10^{11} \text{ cm}^{-2}$  is given by  $V_{ext}/D=4\pi enD/\epsilon_b=4.021 \times 10^4 \text{ V/cm}$ . Here,  $-e$  is the electron charge and  $\epsilon_b=4.5$  is the dielectric constant of  $\text{SiO}_2$ . Since the critical electric field  $E_{cr}$  of the dielectric breakdown for  $\text{SiO}_2$  is  $E_{cr} \approx 10^6 \text{ V/cm}$ , we conclude that the external electric field for the spatially separated electrons and holes is less than the critical electric field for dielectric breakdown in  $\text{SiO}_2$ .

The contributions to the single-electron Hamiltonian from the Zeeman splitting and very small pseudospin splitting (caused by two valleys in graphene) set identically to zero.<sup>29</sup> The 2D Hamiltonian of an isolated electron-hole pair in bilayer graphene with spatially separated electrons ( $e$ ) and holes ( $h$ ) in one valley in magnetic field  $B$  neglecting the Coulomb interaction is given by<sup>29</sup>

$$\hat{H} = v_F \begin{pmatrix} 0 & p_x^{(e)} + ip_y^{(e)} & 0 & 0 \\ p_x^{(e)} - ip_y^{(e)} & 0 & 0 & 0 \\ 0 & 0 & 0 & p_x^{(h)} - ip_y^{(h)} \\ 0 & 0 & p_x^{(h)} + ip_y^{(h)} & 0 \end{pmatrix}, \quad (1)$$

where

$$\mathbf{p}^{(e)} = -i\hbar\nabla_e + \frac{e}{c}\mathbf{A}_e, \quad \mathbf{p}^{(h)} = -i\hbar\nabla_h - \frac{e}{c}\mathbf{A}_h, \quad (2)$$

where  $e$  is an electron charge,  $c$  is the speed of light,  $\mathbf{r}_e$  and  $\mathbf{r}_h$  are 2D vectors of coordinates of electron and hole, respectively,  $\mathbf{A}_e$  and  $\mathbf{A}_h$  are the vector potential of electron and hole, respectively, and  $v_F = \sqrt{3}at/(2\hbar)$  is the Fermi velocity of electrons in graphene ( $a=2.566 \text{ \AA}$  is a lattice constant and  $t \approx 2.71 \text{ eV}$  is the overlap integral between the nearest carbon atoms).<sup>30</sup>

A conserved quantity for an isolated electron-hole pair in magnetic field  $B$  (the exciton magnetic momentum)  $\hat{\mathbf{P}}$  is<sup>13,15,31</sup>

$$\hat{\mathbf{P}} = -i\hbar\nabla_e - i\hbar\nabla_h + \frac{e}{c}(\mathbf{A}_e - \mathbf{A}_h) - \frac{e}{c}[\mathbf{B} \times (\mathbf{r}_e - \mathbf{r}_h)]. \quad (3)$$

The conservation of this quantity is related to the invariance of the system upon a simultaneous translation of  $e$  and  $h$  and gauge transformation. The cylindrical gauge for vector potential is used:  $\mathbf{A}_{e(h)} = 1/2[\mathbf{B} \times \mathbf{r}_{e(h)}]$ .

The eigenfunction of the Hamiltonian [Eq. (1)] of the two-dimensional electron-hole pair  $\psi_\tau$  in the perpendicular magnetic field  $B$ , which is also the eigenfunction of the magnetic momentum  $\hat{\mathbf{P}}$  has the form<sup>13,15,31</sup>

$$\psi_{\mathbf{p}}(\mathbf{R}, \mathbf{r}) = \exp \left[ i \left( \mathbf{P} + \frac{e}{2c} [\mathbf{B} \times \mathbf{r}] \right) \frac{\mathbf{R}}{\hbar} \right] \tilde{\Phi}(\mathbf{r} - \rho_0), \quad (4)$$

where  $\mathbf{R} = (\mathbf{r}_e + \mathbf{r}_h)/2$ , and  $\mathbf{r} = \mathbf{r}_e - \mathbf{r}_h$ , and  $\rho_0 = c[\mathbf{B} \times \mathbf{P}]/(eB^2)$ .

The wave function of the relative coordinate  $\tilde{\Phi}(\mathbf{r})$  can be expressed in terms of the two-dimensional harmonic oscillator eigenfunctions  $\Phi_{n_1, n_2}(\mathbf{r})$ . For an electron in Landau level  $n_+$  and a hole in level  $n_-$ , the four-component wave functions for the relative coordinate are<sup>29</sup>

$$\tilde{\Phi}_{n_+, n_-}(\mathbf{r}) = (\sqrt{2})^{\delta_{n_+, 0} + \delta_{n_-, 0} - 2} \begin{pmatrix} s_+ s_- \Phi_{|n_+|-1, |n_-|-1}(\mathbf{r}) \\ s_+ \Phi_{|n_+|-1, |n_-|}(\mathbf{r}) \\ s_- \Phi_{|n_+|, |n_-|-1}(\mathbf{r}) \\ \Phi_{|n_+|, |n_-|}(\mathbf{r}) \end{pmatrix}, \quad (5)$$

where  $s_{\pm} = \text{sgn}(n_{\pm})$ . The corresponding energy of the electron-hole pair  $E_{n_+, n_-}^{(0)}$  (which is the eigenvalue of the Hamiltonian [Eq. (1)]) is given by<sup>29</sup>

$$E_{n_+, n_-}^{(0)} = \frac{\hbar v_F}{r_B} \sqrt{2} [\text{sgn}(n_+) \sqrt{|n_+|} - \text{sgn}(n_-) \sqrt{|n_-|}], \quad (6)$$

where  $r_B = \sqrt{c\hbar/(eB)}$  is a magnetic length and  $v_F = \sqrt{3}at/(2\hbar)$  is the Fermi velocity of electrons in graphene ( $a=2.566 \text{ \AA}$  is a lattice constant and  $t \approx 2.71 \text{ eV}$  is the overlap integral between the nearest carbon atoms).<sup>30</sup> The two-dimensional harmonic oscillator wave functions eigenfunctions  $\Phi_{n_1, n_2}(\mathbf{r})$  are given by<sup>29</sup>

$$\Phi_{n_1, n_2}(\mathbf{r}) = (2\pi)^{-1/2} 2^{-|m|/2} \frac{\tilde{n}!}{\sqrt{n_1! n_2!} r_B} \frac{1}{r_B^{|m|}} \text{sgn}(m)^m \frac{r^{|m|}}{r_B^{|m|}} \times \exp \left[ -im\phi - \frac{r^2}{4r_B^2} \right] L_{\tilde{n}}^{|m|} \left( \frac{r^2}{2r_B^2} \right), \quad (7)$$

where  $L_{\tilde{n}}^{|m|}$  denotes Laguerre polynomials,  $m = n_1 - n_2$ ,  $\tilde{n} = \min(n_1, n_2)$ , and  $\text{sgn}(m)^m = 1$  for  $m=0$ .

### III. ISOLATED INDIRECT MAGNETOEXCITON

In high magnetic field, the magnetoexciton energy can be calculated by applying the perturbation theory respect to Coulomb electron-hole attraction analogously to 2D quantum wells with nonzero electron and hole masses ( $m_e \neq 0$  and  $m_h \neq 0$ ).<sup>13</sup> This approach allows us to derive the spectrum of isolated indirect magnetoexciton with the spatially separated electron and hole in bilayer graphene. For bilayer graphene, this perturbation theory is valid only for the relatively large separation  $D$  between electron and hole graphene layers and relatively high magnetic fields  $B$  (at  $D \gg r_B$ ) when  $e^2/(\epsilon D) \ll \hbar v_F/r_B$ . Here,  $e^2/(\epsilon D)$  is the characteristic Coulomb electron-hole attraction for the graphene bilayer and  $\hbar v_F/r_B$  is the energy difference between the first and zeroth Landau levels in graphene. The operator of electron-hole Coulomb attraction is

$$\hat{V}(r) = -\frac{e^2}{\epsilon\sqrt{r^2 + D^2}}, \quad (8)$$

where  $\epsilon$  is the dielectric constant of the insulator (SiO<sub>2</sub>) between electron and hole graphene layers and  $D$  is the separation between electron and hole graphene layers.

The magnetoexciton energies  $E_{n_+,n_-}(P)$  in the first order perturbation are equal to

$$E_{n_+,n_-}(P) = E_{n_+,n_-}^{(0)} + \mathcal{E}_{n_+,n_-}(P), \quad (9)$$

where  $E_{n_+,n_-}^{(0)}$  is the unperturbed spectrum given by Eq. (6) and

$$\mathcal{E}_{n_+,n_-}(P) = -\left\langle n_+n_-\mathbf{P} \left| \frac{e^2}{\epsilon\sqrt{D^2 + (r_e - r_h)^2}} \right| n_+n_-\mathbf{P} \right\rangle. \quad (10)$$

For case 1, we calculate the magnetoexciton energy by using the expectation value for an electron in Landau level 1 and a hole in level 1.

In high magnetic field, the magnetoexciton is constructed by electron and hole on the lowest Landau level with the following four-component wave function of the relative coordinate,

$$\tilde{\Phi}_{1,1}(\mathbf{r}) = \frac{1}{2} \begin{pmatrix} \Phi_{0,0}(\mathbf{r}) \\ \Phi_{0,1}(\mathbf{r}) \\ \Phi_{1,0}(\mathbf{r}) \\ \Phi_{1,1}(\mathbf{r}) \end{pmatrix}. \quad (11)$$

Neglecting the transitions between different Landau levels, the first order perturbation respect to Coulomb attraction results in the following expression for the energy of magnetoexciton:

$$E_{1,1}(P) = \mathcal{E}_{1,1}(P) = -\left\langle 1,1,\mathbf{P} \left| \frac{e^2}{\epsilon\sqrt{D^2 + (r_e - r_h)^2}} \right| 1,1,\mathbf{P} \right\rangle. \quad (12)$$

Denoting the averaging by the two-dimensional harmonic oscillator eigenfunctions  $\Phi_{n_1,n_2}(\mathbf{r})$  [Eq. (7)] as  $\langle\langle \tilde{n}m\mathbf{P} | \cdots | \tilde{n}m\mathbf{P} \rangle\rangle$  [ $\tilde{n}$  and  $m$  are defined below, Eq. (7)], we get the energy of an indirect magnetoexciton created by the spatially separated electron and hole on the lowest Landau level,

$$\begin{aligned} E_{1,1}(P) &= \langle 1,1,\mathbf{P} | \hat{V}(r) | 1,1,\mathbf{P} \rangle \\ &= \langle\langle 0,0,\mathbf{P} | \hat{V}(r) | 0,0,\mathbf{P} \rangle\rangle + \langle\langle 0,1,\mathbf{P} | \hat{V}(r) | 0,1,\mathbf{P} \rangle\rangle \\ &\quad + \langle\langle 0,1,\mathbf{P} | \hat{V}(r) | 0,1,\mathbf{P} \rangle\rangle + \langle\langle 1,0,\mathbf{P} | \hat{V}(r) | 1,0,\mathbf{P} \rangle\rangle. \end{aligned} \quad (13)$$

Substituting for small magnetic momenta  $P \ll \hbar/r_B$  and  $P \ll \hbar D/r_B^2$  the following relations:<sup>17</sup>

$$\langle\langle \tilde{n}m\mathbf{P} | \hat{V}(r) | \tilde{n}m\mathbf{P} \rangle\rangle = \mathcal{E}_{\tilde{n}m}^{(b)} + \frac{P^2}{2M_{\tilde{n}m}(B,D)} \quad (14)$$

into Eq. (13), we get the dispersion law of a magnetoexciton for small magnetic momenta,

$$\begin{aligned} E_{1,1}(P) &= \mathcal{E}_{00}^{(b)}(B,D) + 2\mathcal{E}_{01}^{(b)}(B,D) + \mathcal{E}_{10}^{(b)}(B,D) \\ &\quad + \left( \frac{1}{M_{00}(B,D)} + \frac{2}{M_{01}(B,D)} + \frac{1}{M_{10}(B,D)} \right) \frac{P^2}{2} \\ &= \mathcal{E}_B^{(b)}(D) + \frac{P^2}{2m_B(D)}, \end{aligned} \quad (15)$$

where the binding energy  $\mathcal{E}_B^{(b)}(D)$  and the effective magnetic mass  $m_B(D)$  of a magnetoexciton with spatially separated electron and hole in bilayer graphene are

$$\begin{aligned} \mathcal{E}_B^{(b)}(D) &= \mathcal{E}_{00}^{(b)}(B,D) + 2\mathcal{E}_{01}^{(b)}(B,D) + \mathcal{E}_{10}^{(b)}(B,D), \\ \frac{1}{m_B(D)} &= \frac{1}{M_{00}(B,D)} + \frac{2}{M_{01}(B,D)} + \frac{1}{M_{10}(B,D)}, \end{aligned} \quad (16)$$

where constants  $\mathcal{E}_{00}^{(b)}(B,D)$ ,  $\mathcal{E}_{01}^{(b)}(B,D)$ ,  $\mathcal{E}_{10}^{(b)}(B,D)$ ,  $M_{00}(B,D)$ ,  $M_{01}(B,D)$ , and  $M_{10}(B,D)$  depending on magnetic field  $B$  and the interlayer separation  $D$  are given in Ref. 17,

$$\mathcal{E}_{00}^{(b)}(B,D) = -\mathcal{E}_0 \exp\left[\frac{D^2}{2r_B^2}\right] \operatorname{erfc}\left[\frac{D}{\sqrt{2}r_B}\right],$$

$$\begin{aligned} \mathcal{E}_{01}^{(b)}(B,D) &= -\mathcal{E}_0 \left[ \left( \frac{1}{2} - \frac{D^2}{2r_B^2} \right) \exp\left[\frac{D^2}{2r_B^2}\right] \operatorname{erfc}\left[\frac{D}{\sqrt{2}r_B}\right] \right. \\ &\quad \left. + \frac{D}{\sqrt{2\pi}r_B} \right], \end{aligned}$$

$$\begin{aligned} \mathcal{E}_{10}^{(b)}(B,D) &= -\mathcal{E}_0 \left[ \left( \frac{3}{4} + \frac{D^2}{2r_B^2} + \frac{D^4}{4r_B^4} \right) \exp\left[\frac{D^2}{2r_B^2}\right] \operatorname{erfc}\left[\frac{D}{\sqrt{2}r_B}\right] \right. \\ &\quad \left. - \frac{D}{2\sqrt{2\pi}r_B} - \left( \frac{D}{\sqrt{2}r_B} \right)^3 \frac{1}{\sqrt{\pi}} \right], \end{aligned}$$

$$\begin{aligned} M_{00}(B,D) &= M_0 \left[ \left( 1 + \frac{D^2}{r_B^2} \right) \exp\left[\frac{D^2}{2r_B^2}\right] \operatorname{erfc}\left[\frac{D}{\sqrt{2}r_B}\right] \right. \\ &\quad \left. - \sqrt{\frac{2D}{\pi r_B}} \right]^{-1}, \end{aligned}$$

$$\begin{aligned} M_{01}(B,D) &= M_0 \left[ \left( 3 + \frac{D^2}{r_B^2} \right) \frac{D}{\sqrt{2\pi}r_B} - \left( \frac{1}{2} + 2\frac{D^2}{r_B^2} \right) \right. \\ &\quad \left. + \frac{D^4}{2r_B^4} \right] \exp\left[\frac{D^2}{2r_B^2}\right] \operatorname{erfc}\left[\frac{D}{\sqrt{2}r_B}\right]^{-1}, \end{aligned}$$

$$M_{10}(B, D) = M_0 \left[ \frac{1}{4} \left( 7 + 25 \frac{D^2}{r_B^2} + 11 \frac{D^4}{r_B^4} + \frac{D^6}{r_B^6} \right) \times \exp \left[ \frac{D^2}{2r_B^2} \right] \operatorname{erfc} \left[ \frac{D}{\sqrt{2}r_B} \right] - \left( \frac{17}{2} + 5 \frac{D^2}{r_B^2} + \frac{D^4}{2r_B^4} \right) \frac{D}{\sqrt{2\pi}r_B} \right]^{-1}, \quad (17)$$

where constants  $\mathcal{E}_0$  and  $M_0$  and function  $\operatorname{erfc}(z)$  are defined as<sup>17</sup>

$$\mathcal{E}_0 = \left\langle \left\langle 00\mathbf{P} \left| \frac{e^2}{\epsilon|\mathbf{r}|} \right| 00\mathbf{P} \right\rangle \right\rangle_{\mathbf{P}=0} = \frac{e^2}{\epsilon r_B} \sqrt{\frac{\pi}{2}},$$

$$M_0 = - \left[ 2 \left( \left\langle \left\langle 00\mathbf{P} \left| \frac{e^2}{\epsilon|\mathbf{r}|} \right| 00\mathbf{P} \right\rangle \right\rangle - \mathcal{E}_0 \right) \right]^{-1} P^2 = \frac{2^{3/2} \epsilon \hbar^2}{\sqrt{\pi} e^2 r_B},$$

$$\operatorname{erfc}(z) = \frac{2}{\sqrt{\pi}} \int_z^{+\infty} \exp(-t^2) dt. \quad (18)$$

For case 2, we calculate the magnetoexciton energy by using the expectation value for an electron in Landau level 1 and a hole in level 0. We have  $E_{1,0}(P) = \langle 0, 0, \mathbf{P} | \hat{V}(r) | 0, 0, \mathbf{P} \rangle + \langle 0, 1, \mathbf{P} | \hat{V}(r) | 0, 1, \mathbf{P} \rangle$ .

Since below we will be interested in the description of magnetoexcitonic gas as a 2D dilute gas of weakly interacting bosons with pair dipole-dipole repulsion, we consider bilayer graphene structure with relatively large interlayer separation  $D \gg r_B$  with the corresponding magnetoexcitonic binding energy  $\mathcal{E}_B^{(b)}(D)$  and effective magnetic mass  $m_B(D)$  defined according to Eq. (15) by using the following constants:

$$\mathcal{E}_{\tilde{n}\tilde{m}}^{(b)}(B, D) = - \frac{e^2}{\epsilon D} \left( 1 - \frac{l_{\tilde{n}\tilde{m}}^2}{2D^2} \right),$$

$$M_{\tilde{n}\tilde{m}}(B, D) = \frac{\sqrt{\pi} D^3}{2^{3/2} r_B^3} M_0 \left( 1 - \frac{3l_{\tilde{n}\tilde{m}}^2}{2D^2} \right)^{-1}, \quad (19)$$

where  $l_{\tilde{n}\tilde{m}}^2 = \langle \langle \tilde{n}\tilde{m}\mathbf{P} | r^2 | \tilde{n}\tilde{m}\mathbf{P} \rangle \rangle_{\mathbf{P}=0}$  and  $(l_{00}^2 = 2r_B^2, l_{01}^2 = 4r_B^2, l_{10}^2 = 6r_B^2)$ . The 2D radius of magnetoexciton on the lowest Landau level for the case 1 is given by

$$r_{1,1}^2(P=0) = \langle 1, 1, \mathbf{P} | r^2 | 1, 1, \mathbf{P} \rangle_{\mathbf{P}=0} = l_{00}^2 + 2l_{01}^2 + l_{10}^2 = 16r_B^2,$$

$$r_{1,1} = 4r_B. \quad (20)$$

Substitution Eq. (19) into Eq. (16) gives the binding energy  $\mathcal{E}_B^{(b)}(D)$  and the effective magnetic mass  $m_B(D)$  of the indirect magnetoexciton for the case 1 at  $D \gg r_B$  in bilayer graphene in high magnetic field,

$$\mathcal{E}_B^{(b)}(B, D) = - \frac{e^2}{\epsilon D} \left( 4 - \frac{l_{00}^2 + 2l_{01}^2 + l_{10}^2}{2D^2} \right) = - \frac{4e^2}{\epsilon D} \left( 1 - \frac{2r_B^2}{D^2} \right),$$

$$m_B(D) = \frac{\sqrt{\pi} D^3}{2^{3/2} r_B^3} M_0 \left( 4 - \frac{3(l_{00}^2 + 2l_{01}^2 + l_{10}^2)}{2D^2} \right)^{-1}$$

$$= \frac{1}{8} \sqrt{\frac{\pi} {2}} \frac{D^3}{r_B^3} M_0 \left( 1 - \frac{6r_B^2}{D^2} \right)^{-1} = \frac{\hbar^2 \epsilon D^3}{4e^2 r_B^4} \left( 1 - \frac{6r_B^2}{D^2} \right)^{-1}. \quad (21)$$

In the limit of very large interlayer separation  $D \gg r_B$  for case 1, the asymptotical values of the binding energy  $\mathcal{E}_B^{(b)}(D)$  and the effective magnetic mass  $m_B(D)$  of an indirect magnetoexciton in bilayer graphene are

$$\mathcal{E}_B^{(b)}(B, D) = - \frac{4e^2}{\epsilon D}, \quad m_B(D) = \frac{\epsilon}{4c^2} D^3 B^2. \quad (22)$$

We can see that the effective magnetic mass of indirect magnetoexciton is approximately four times lower in bilayer graphene than in CQWs at the same  $D$ ,  $\epsilon$ , and  $\mathbf{B}$  (compare Eq. (22) to Ref. 17). The magnetoexcitonic energy is approximately four times higher in bilayer graphene than in CQWs at the same  $D$ ,  $\epsilon$ , and  $\mathbf{B}$ .

Counting energy from the binding energy of magnetoexciton, the dispersion relation  $\epsilon_k(P)$  of isolated magnetoexciton is a quadratic function at small magnetic momenta  $P \ll \hbar/r_B$  and  $P \ll \hbar D/r_B^2$ ,

$$\epsilon_k(\mathbf{P}) = \frac{P^2}{2m_{Bk}}, \quad (23)$$

where  $m_{Bk}$  is the effective magnetic mass, which dependent on  $B$  and the distance  $D$  between electron and hole layers and quantum number  $k$  [where  $k=(n_+, n_-)$  are the magnetoexcitonic quantum numbers].

By using the Feynman theorem (we denote  $\langle Pk | \dots | Pk \rangle$  as  $\langle \dots \rangle$ ), one can obtain for isolated magnetoexciton velocity  $\mathbf{v}$  the following expression:<sup>31</sup>

$$\mathbf{v} = \langle \hat{\mathbf{v}} \rangle = \left\langle \frac{\partial \hat{H}}{\partial \mathbf{P}} \right\rangle = \frac{\partial \epsilon_k(P)}{\partial \mathbf{P}} = \frac{\mathbf{P}}{m_{Bk}}. \quad (24)$$

In the limit of large excitonic magnetic momenta  $P \gg \hbar/r_B$  and  $P \gg \hbar D/r_B^2$  substituting the following relations:<sup>17</sup>

$$\langle \langle \tilde{n}\tilde{m}\mathbf{P} | \hat{V}(r) | \tilde{n}\tilde{m}\mathbf{P} \rangle \rangle = - \frac{\hbar e^2}{\epsilon P r_B^2} \left[ 1 - \left( D^2 - \frac{l_{\tilde{n}\tilde{m}}^2}{2} \right) \frac{\hbar^2}{2r_B^4 P^2} \right] \quad (25)$$

into Eq. (13), we obtain the asymptotic of the magnetoexcitonic dispersion law at large magnetic momenta,

$$E_{1,1}(P) = - \frac{\hbar e^2}{\epsilon P r_B^2} \left[ 4 - \left( 4D^2 - \frac{l_{00}^2 + 2l_{01}^2 + l_{10}^2}{2} \right) \frac{\hbar^2}{2r_B^4 P^2} \right]$$

$$= - \frac{4\hbar e^2}{\epsilon P r_B^2} \left[ 1 - \left( D^2 - 2r_B^2 \right) \frac{\hbar^2}{2r_B^4 P^2} \right]. \quad (26)$$

Analogously to case 1, for case 2, by applying  $E_{1,1}(P)$  instead of  $E_{1,0}(P)$  in Eq. (13), we obtain the binding energy  $\mathcal{E}_B^{(b)}(D)$  and the effective magnetic mass  $m_B(D)$  of a magnetoexciton with spatially separated electron and hole in two-layer graphene as  $\mathcal{E}_B^{(b)}(D) = \mathcal{E}_{00}^{(b)}(B, D) + \mathcal{E}_{01}^{(b)}(B, D)$  and  $m_B^{-1}(D) = M_{00}^{-1}(B, D) + M_{01}^{-1}(B, D)$ . The radius of a magnetoexciton in the lowest Landau level is given by  $r_{1,0}(B) = \sqrt{6}r_B$ .

For case 1 for large interlayer separation  $D \gg r_B$ , the asymptotic values of the binding energy  $\mathcal{E}_B^{(b)}(D)$  and the effective magnetic mass  $m_B(D)$  are  $\mathcal{E}_B^{(b)}(B, D) = -4e^2/(\epsilon_b D)$ , and  $m_B(D) = \epsilon_b D^3 B^2 / (4c^2)$ . When  $D \ll r_B$ , these quantities denoted by  $\mathcal{E}_0$  and  $M_0$  are presented above. We can see that the effective magnetic mass of an indirect magnetoexciton is approximately four times smaller than in CQWs at the same  $D$ ,  $\epsilon_b$ , and  $\mathbf{B}$ .<sup>17</sup> The magnetoexcitonic energy is approximately four times larger in two-layer graphene than in CQWs. For case 2 for large interlayer separation  $D \gg r_B$ , the asymptotic values of the binding energy  $\mathcal{E}_B^{(b)}(D)$  and the effective magnetic mass  $m_B(D)$  are  $\mathcal{E}_B^{(b)}(B, D) = -2e^2/(\epsilon_b D)$  and  $m_B(D) = \epsilon_b D^3 B^2 / (2c^2)$ . For case 2, we can see that the effective magnetic mass of an indirect magnetoexciton is approximately two times smaller than in CQWs at the same  $D$ ,  $\epsilon_b$ , and  $\mathbf{B}$ .<sup>17</sup> The magnetoexcitonic energy is approximately two times larger in two-layer graphene than in CQWs.

#### IV. COLLECTIVE PROPERTIES OF DIPOLE MAGNETOEXCITONS IN BILAYER GRAPHENE

Due to interlayer separation  $D$  indirect magnetoexcitons both in ground state and in excited states have electrical dipole moments. We suppose that indirect exciton interact as *parallel* dipoles. This is valid, when  $D$  is larger than the mean separation  $\langle r \rangle$  between electron and hole along graphene layers  $D \gg \langle r \rangle$ . We take into account that at high magnetic fields  $\langle r \rangle \approx Pr_B^2/\hbar$  ( $\langle \mathbf{r} \rangle$  is normal to  $\mathbf{P}$ ) and that the typical value of magnetic momenta [with exactness to logarithm of the exciton density,  $\log(n)$ , see below] is  $P \sim \hbar \sqrt{n}$ , where  $n$  is two-dimensional density of magnetoexcitons. So, the inequality  $D \gg \langle r \rangle$  is valid at  $D \gg \sqrt{nr_B^2}$ .

Since electrons on a graphene lattice can be in two valleys, there are four types of exciton in bilayer graphene. Due to the fact that all these types of exciton have identical envelope wave functions and energies,<sup>29</sup> we consider below only exciton in one valley. Also, we use  $n_0 = n/(4s)$  as the density of exciton in one layer, with  $n$  denoting the total density of exciton and  $s$  is the spin degeneracy (equal to 4 for magnetoexcitons in bilayer graphene).

The distinction between exciton and bosons manifests itself in exchange effects.<sup>11,12,32,33</sup> These effects for exciton with spatially separated  $e$  and  $h$  in a dilute system  $na^2(B, D) \ll 1$  are suppressed due to the negligible overlapping of wave functions of two exciton on account of the potential barrier, which is associated with the dipole-dipole repulsion of indirect exciton<sup>11</sup> [here,  $a(B, D)$  is the magnetoexciton radius along graphene layers]. Two indirect exciton in a dilute system interact as  $U(R) = e^2 D^2 / (\epsilon R^3)$ , where  $R$  is the distance between exciton dipoles along the graphene layers. Small tunneling parameter connected with this barrier is

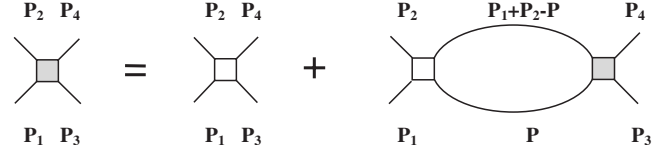


FIG. 2. The equation for the vertex  $\Gamma$  in the representation of magnetic momenta  $\mathbf{P}$  and quantum numbers  $n_+$  and  $n_-$ .

$$\exp \left[ -\frac{1}{\hbar} \int_{a(B,D)}^{r_0} \sqrt{2m_{Bk} \left( \frac{e^2 D^2}{\epsilon R^3} - \frac{\kappa^2}{2m_{Bk}} \right)} dR \right],$$

where

$$\kappa^2 \sim \hbar^2 \frac{n}{s \log[s \hbar^4 \epsilon^2 / (2\pi n m_{Bk}^2 e^4 D^4)]}$$

is the characteristic momentum of the system (see below) and  $r_0 = (2m_{Bk} e^2 D^2 / \kappa^2)^{1/3}$  is the classical turning point for the dipole-dipole interaction. In high magnetic fields, the small parameter mentioned above has the form  $\exp[-2\hbar^{-1}(m_{Bk})^{1/2} e D a^{-1/2}(B, D)]$ . So, at zero temperature  $T=0$ , the dilute gas of magnetoexcitons, which is a boson system, form the Bose-Einstein condensate.<sup>34,35</sup> Therefore, the system of indirect magnetoexcitons can be treated by the diagram technique for a boson system.

In contrast to a 2D boson system in the absence of magnetic field,<sup>36</sup> due to nonseparation of the relative motion of  $e$  and  $h$  and the motion of magnetoexciton as a whole in magnetic fields [Eq. (4)], the Green's functions depend on both the external coordinates  $\mathbf{R}$  and  $\mathbf{R}'$  and the internal coordinates  $\mathbf{r}$  and  $\mathbf{r}'$ .

For the dilute two-dimensional magnetoexciton system [ $na^2(B, D) \ll 1$ ], the summation of ladder diagrams is adequate. The integral equation for vertex  $\Gamma$  in the ladder approximation is represented in Fig. 2. In the strong magnetic fields, the representation by using as a basis of isolated magnetoexciton wave functions  $\psi_{\mathbf{P}, n_+, n_-}(\mathbf{r}, \mathbf{R})$  given by Eq. (4) is convenient.

We use the following approximation for the interaction between two magnetoexcitons  $U(P) = U_0$  at  $P < \hbar a^{-1}(B, D)$  and  $U(P) = 0$  at  $P > \hbar a^{-1}(B, D)$ . After exciton-exciton scattering, their total magnetic momentum is conserved, but magnetic momentum of each exciton can be changed. Since the mean distance between  $e$  and  $h$  along graphene layers is proportional to the magnetic momentum, the scattering is accompanied by the exciton polarization. We consider sufficiently low temperatures when magnetoexciton states with only small magnetic momenta  $P \ll \hbar/r_B$  are filled. The change of these magnetic momenta due to exciton-exciton scattering is also negligible due to the conservation of the total magnetic momentum. However, these small magnetic momenta correspond to small separation between electrons and holes along graphene layers  $r \ll r_B$ . So, magnetoexciton polarization due to scattering is negligible and the magnetoexciton dipole moment keeps to be almost normal to graphene layers  $d = eD$ , i.e., the interexciton interaction law is not changed due to the scattering.

The equation for  $\Gamma$  can be solved in the strong magnetic fields  $e^2/(\epsilon D) \ll \hbar v_F/r_B$ , when the characteristic value of  $e$ - $h$  separation in the magnetoexciton  $|\langle \mathbf{r} \rangle|$  has the order of the magnetic length  $r_B = \sqrt{\hbar/(eB)}$ . The functions  $\tilde{\Phi}_k(\mathbf{P}, \mathbf{r})$  [see Eq. (4)] are dependent on the difference  $(\mathbf{r} - \rho_0)$ , where  $\rho_0 = (r_B^2/B)[\mathbf{B} \times \mathbf{P}]$ . At small magnetic momenta  $P \ll \hbar/r_B$ , we have  $\rho_0 \ll r_B$ , and, therefore, in functions  $\tilde{\Phi}_k(\mathbf{r} - \rho_0)$ , we can ignore the variable  $\rho_0$  compare to  $\mathbf{r}$ . In the strong magnetic field, quantum numbers  $k$  correspond to the quantum numbers  $(n_+, n_-)$  (see above). For the lowest Landau level, we denote for case 1  $\varepsilon_{11}(\mathbf{P}) = \varepsilon(\mathbf{P})$  and for case 2  $\varepsilon_{10}(\mathbf{P}) = \varepsilon(\mathbf{P})$ . By using the orthonormality of the four-component wave functions of the relative coordinate for a noninteracting pair of an electron in Landau level  $n_+$  and a hole in level  $n_-$  [ $\tilde{\Phi}_{n_+, n_-}(\mathbf{P} = \mathbf{0}, \mathbf{r})$ ],<sup>29</sup> we obtain an approximate equation for the vertex  $\Gamma$  in strong magnetic fields. Due to the orthonormality of the four-component wave functions  $\tilde{\Phi}_{n_+, n_-}(\mathbf{0}, \mathbf{r})$ , the projection of the equation for the vertex in the ladder approximation for a dilute system onto the lowest Landau level results in the scalar integral equation, which does not reflect the spinor nature of the four-component magnetoexcitonic wave functions in graphene. In high magnetic field, one can ignore transitions between Landau levels and consider only the lowest Landau level states in case 1  $n_+ = n_- = 1$  and in the case 2  $n_+ = 1; n_- = 0$ . Since typically the value of  $r$  is  $r_B$  and  $P \ll \hbar/r_B$  in this approximation, the equation for the vertex in the magnetic momentum representation  $P$  for the lowest Landau level (for graphene layers in case 1  $n_+ = n_- = 1$  and in case 2  $n_+ = 1; n_- = 0$ ) has the same form (compare to Ref. 5) as for a 2D boson system in the absence of magnetic field, but with the magnetoexciton magnetic mass  $m_B$  (which depends on  $B$  and  $D$ ) instead of the exciton mass ( $M = m_e + m_B$ ) and magnetic momentum instead of inertial momentum,

$$\begin{aligned} \Gamma(\mathbf{p}, \mathbf{p}'; P) &= U(\mathbf{p} - \mathbf{p}') \\ &+ s \int \frac{d^2 q}{(2\pi\hbar)^2} \frac{U(\mathbf{p} - \mathbf{q})\Gamma(\mathbf{q}, \mathbf{p}'; P)}{\kappa^2 + \Omega - \frac{\mathbf{P}^2}{4m_B} - \frac{q^2}{m_B} + i\delta}, \\ \delta &\rightarrow +0, \\ \mu &= \frac{\kappa^2}{2m_B} = n_0\Gamma_0 = n_0\Gamma(0, 0; 0), \end{aligned} \quad (27)$$

where  $P = \{\mathbf{P}, \Omega\}$  and  $\mu$  is the chemical potential of the system.

The specific feature of two-dimensional Bose system is connected with logarithmic divergence of two-dimensional scattering amplitude at zero energy.<sup>11,12,36</sup> A simple analytical solution of Eq. (27) for the chemical potential can be obtained if  $\kappa m_B e^2 D^2 / (\hbar^3 \epsilon) \ll 1$ . In strong magnetic fields at  $D \gg r_B$  according to Eq. (21), the exciton magnetic mass is defined as  $m_B \approx \hbar^2 \epsilon D^3 / (4e^2 r_B^4)$ . So, the inequality  $\kappa m_B e^2 D^2 / (\hbar^3 \epsilon) \ll 1$  is valid if  $D \ll (r_B^4 / n^{1/2})^{1/5}$ . As a result, the chemical potential  $\mu$  is obtained in the form

$$\mu = \frac{\kappa^2}{2m_B} = \frac{\pi \hbar^2 n}{sm_B \log[s \hbar^4 \epsilon^2 / (2\pi m_B^2 e^4 D^4)]}. \quad (28)$$

The solution of Eq. (27) at small magnetic momenta corresponds to the sound spectrum of collective excitations  $\varepsilon(P) = c_s P$  with the sound velocity  $c_s = \sqrt{\Gamma n / (4sm_B)} = \sqrt{\mu / m_B}$ , where  $\mu$  is defined by Eq. (28). Since magnetoexcitons have a sound spectrum of collective excitations at small magnetic momenta  $P$  due to the dipole-dipole repulsion, the magnetoexcitonic superfluidity is possible at small temperatures  $T$  in bilayer graphene because the sound spectrum satisfies to the Landau criterion of superfluidity.<sup>34,35</sup>

It can be shown that the interaction between two magnetoexcitons on the lowest Landau level can be neglected in strong magnetic field at  $D=0$  analogously to Ref. 13. The dipole moment of each exciton at is  $\mathbf{d}_{1,2} = e\rho_0 = r_B^2[\mathbf{B} \times \mathbf{P}_{1,2}]/B$  [see Eq. (4)], where  $\mathbf{P}_1$  and  $\mathbf{P}_2$  are the magnetic momenta of each exciton and  $P_1, P_2 \ll 1/r_B$ . The magnetoexcitons are located at a distance  $R \gg r_B$  from each other. The corresponding contribution to the energy of their dipole-dipole interaction is  $\sim E_b(r_B/R)^3 P_1 P_2 r_B^2 / \epsilon \sim (r_B/R)^3 P_1 P_2 / (\epsilon M_0)$ . Applying for the radius of magnetoexciton in bilayer graphene  $r_{1,1} = 4r_B$  given by Eq. (20), the van der Waals attraction of the exciton at zero momenta are proportional to  $\sim (r_B/R)^6$ . Therefore, at  $D=0$  in the limit of the strong magnetic field for dilute system  $r_B \ll R$ , both the dipole-dipole interaction and the van der Waals attraction vanish, and magnetoexcitons form an ideal Bose gas analogously to Ref. 13. So, at  $D=0$  and  $T=0$ , there is BEC of the ideal magnetoexcitonic gas. There is no superfluidity at  $D=0$  because the quadratic spectrum of noninteracting magnetoexcitons given by Eq. (23) does not satisfy to the Landau criterion of superfluidity. For the system with spatially separated electrons and hole at  $D \gg r_B$ , the superfluidity appears because the pair dipole-dipole interaction  $U(R) = e^2 D^2 / \epsilon R^3$  and magnetoexcitonic dipole moment  $d = eD$  do not depend on magnetic field  $B$  (see above).

## V. SUPERFLUIDITY OF DIPOLE MAGNETOEXCITONS IN BILAYER GRAPHENE

The magnetoexcitons that are constructed by spatially separated electrons and holes in bilayer graphene at large interlayer separations  $D \gg r_B$  form two-dimensional weakly nonideal gas of bosons with the pair dipole-dipole repulsion. So, the phase transition superfluid-normal phase in this system is the Kosterlitz-Thouless transition.<sup>37</sup> The temperature of the Kosterlitz-Thouless transition  $T_c$  to the superfluid state in a two-dimensional magnetoexciton system is determined by

$$T_c = \frac{\pi \hbar^2 n_s(T_c)}{2k_B m_B}, \quad (29)$$

where  $n_s(T)$  is the superfluid density of the magnetoexciton system as a function of temperature  $T$ , magnetic field  $B$  and interlayer distance  $D$ , and  $k_B$  is the Boltzmann constant.

The function  $n_s(T)$  [Eq. (29)] can be found from the relation  $n_s = n / (4s) - n_n$  (where  $n$  is the total density and  $n_n$  is the normal component density). We determine the normal com-

ponent density by the usual procedure.<sup>34</sup> Suppose that the magnetoexciton system moves with a velocity  $\mathbf{u}$ . At nonzero temperatures  $T$ , dissipating quasiparticles will appear in this system. Since their density is small at low temperatures, one can assume that the gas of quasiparticles is an ideal Bose gas. To calculate the superfluid component density, we find the total current of quasiparticles in a frame in which the superfluid component is at rest. Then, by using Eq. (24), we obtain the mean total current of 2D magnetoexcitons in the coordinate system, moving with a velocity  $\mathbf{u}$ ,

$$\langle \mathbf{J} \rangle = \frac{1}{m_B} \langle \mathbf{P} \rangle = \frac{s}{m_B} \int \frac{d\mathbf{P}}{(2\pi\hbar)^2} \mathbf{P} f[\varepsilon(P) - \mathbf{P}\mathbf{u}], \quad (30)$$

where  $f[\varepsilon(P)] = (\exp[\varepsilon(P)/(k_B T)] - 1)^{-1}$  is the Bose-Einstein distribution function. Expanding the expression inside the integral in the first order by  $\mathbf{P}\mathbf{u}/(k_B T)$ , we have

$$\langle \mathbf{J} \rangle = -s \frac{\mathbf{u}}{2m_B} \int \frac{d\mathbf{P}}{(2\pi\hbar)^2} P^2 \frac{\partial f[\varepsilon(P)]}{\partial \varepsilon} = \frac{3\zeta(3)s k_B^3 T^3}{2\pi\hbar^2 m_B c_s^4} \mathbf{u}, \quad (31)$$

where  $\zeta(z)$  is the Riemann zeta function [ $\zeta(3) \approx 1.202$ ]. Then, we define the normal component density  $n_n$  as<sup>34</sup>

$$\langle \mathbf{J} \rangle = n_n \mathbf{u}. \quad (32)$$

By comparing Eqs. (32) and (31), we obtain the expression for the normal density  $n_n$ . Consequently, we have for the superfluid density,

$$n_s = n/(4s) - n_n = n/(4s) - \frac{3\zeta(3) k_B^3 T^3}{2\pi\hbar^2 c_s^4 m_B}. \quad (33)$$

It turns out that the expression for the superfluid density  $n_s$  in the strong magnetic field for the magnetoexciton rare system differs from analogous expression in the absence of magnetic field in semiconductor CQWs (compare to Refs. 11 and 12) by replacing the total exciton mass  $M = m_e + m_B$  with the magnetoexciton exciton magnetic mass  $m_B$  taken from Eq. (16).

In a 2D system, superfluidity of magnetoexcitons appears below the Kosterlitz-Thouless transition temperature [Eq. (29)], where only coupled vortices are present.<sup>37</sup> By using Eq. (33) for the density  $n_s$  of the superfluid component, we obtain an equation for the Kosterlitz-Thouless transition temperature  $T_c$ . Its solution is

$$T_c = \left[ \left( 1 + \sqrt{\frac{32}{27} \left( \frac{s m_B k_B T_c^0}{\pi\hbar^2 n} \right)^3 + 1} \right)^{1/3} - \left( \sqrt{\frac{32}{27} \left( \frac{s m_B k_B T_c^0}{\pi\hbar^2 n} \right)^3 + 1} - 1 \right)^{1/3} \right] \frac{T_c^0}{2^{1/3}}. \quad (34)$$

Here,  $T_c^0$  is an auxiliary quantity, which is equal to the temperature at which the superfluid density vanishes in the mean-field approximation (i.e.,  $n_s(T_c^0) = 0$ ),

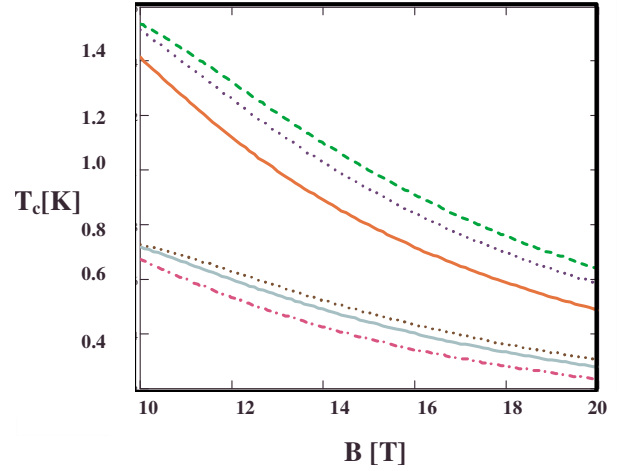


FIG. 3. (Color online) Dependence of Kosterlitz-Thouless transition temperature  $T_c = T_c(B)$  (in units of kelvins) versus magnetic field for two-layer graphene separated by  $\text{SiO}_2$ , with  $\epsilon_b = 4.5$ . The magnetoexciton density  $n = 4 \times 10^{11} \text{ cm}^{-2}$ . Different interlayer separations  $D$  are chosen for case 1:  $D = 30 \text{ nm}$  (solid curve),  $D = 28 \text{ nm}$  (dotted curve), and  $D = 27 \text{ nm}$  (dashed curve). For case 2:  $D = 30 \text{ nm}$  (dashed-dotted curve),  $D = 28 \text{ nm}$  (thin solid curve), and  $D = 27 \text{ nm}$  (thin dotted curve).

$$T_c^0 = \frac{1}{k_B} \left( \frac{\pi\hbar^2 n c_s^4 m_B}{6s\zeta(3)} \right)^{1/3}. \quad (35)$$

The temperature  $T_c^0 = T_c^0(B, D)$  may be used as a crude estimate of the crossover region where local superfluid density appears for rare magnetoexciton system on the scales smaller or of order of mean intervortex separation in the system. The local superfluid density can manifest itself in local optical properties or local transport properties.

According to Eqs. (34) and (35), the temperature of the onset of superfluidity due to the Kosterlitz-Thouless transition at a fixed magnetoexciton density  $T_c$  decreases as a function of magnetic field  $B$  and interlayer separation  $D$  due to the increase in  $m_B$  as a function of  $B$  and  $D$  [see Eq. (21)].  $T_c$  decreases as  $B^{-1/2}$  at  $D \ll r_B$  or as  $B^{-2}$  at  $D \gg r_B$ .

The dependence of  $T_c$  on  $B$  and  $D$  for cases 1 and 2 is represented in Fig. 3 (since in case 1, the binding energy two times higher and the effective magnetic mass is two times smaller than in case 2, the magnetoexcitons in case 1 are expected to be twice more stable and  $T_c$  in case 1 is expected to be approximately twice higher than in case 2 at fixed  $n$ ,  $D$  and  $B$ ). According to Eq. (34), the temperature  $T_c$  for the onset of superfluidity due to the Kosterlitz-Thouless transition at a fixed magnetoexciton density decreases as a function of magnetic field  $B$  and interlayer separation  $D$ . This is due to the increased  $m_B$  as a function of  $B$  and  $D$ .  $T_c$  decreases as  $B^{-1/2}$  at  $D \ll r_B$  or as  $B^{-2}$  when  $D \gg r_B$ .

We note that, according to Eq. (34), the Kosterlitz-Thouless transition temperature is presented above as a function of the density of excitons. The calculation carried out at fixed density which leads to Eq. (34) is appropriate only for optically generated metastable indirect exciton (case 2). For local pairs of “exciton” created by biasing the two-layer

structure (case 1), the chemical potential is fixed rather than the density. In this case, the chemical potential of the exciton can be controlled by changing the external electric field. The Kosterlitz-Thouless transition temperature for case 2 can also be determined by Eqs. (34) and (35) if we replace  $n$  by the following expression  $n \approx sm_B \mu / (\pi \hbar^2)$ , which comes from a numerical estimate obtained from Eq. (28), i.e.,  $\mu \approx \pi \hbar^2 n / (14 sm_B)$ . The denominator on the right-hand side of Eq. (28) depends on  $n$  very weakly for the densities in the range from  $10^{10}$  to  $4 \times 10^{11} \text{ cm}^{-2}$ .

According to Eq. (26), for large magnetic momenta  $P$ , the isolated magnetoexciton spectrum  $\varepsilon(P)$  contrary to the case  $H=0$  has a constant limit (we count energy from the magnetoexcitonic binding energy  $E_b$ ) given by

$$\varepsilon(P) \sim 4 \sqrt{\frac{\pi}{2}} \frac{e^2}{\epsilon r_B} - \frac{4 \hbar e^2}{\epsilon P r_B^2}, \quad D \ll a(B, D), \quad P r_B^2 \gg D,$$

$$\varepsilon(P) \sim \frac{4e^2}{\epsilon D} - \frac{4 \hbar e^2}{\epsilon P r_B^2}, \quad D \gg a(B, D), \quad P r_B^2 \gg D. \quad (36)$$

Consequently, the spectrum of *interacting* magnetoexciton system also have a plateau at great momenta. So, Landau criterion of superfluidity is not valid at large  $P$  for the interacting magnetoexciton system. However, the probability of excitation of quasiparticles with magnetic momenta  $P \gg 1/r_B$  by moving magnetoexciton system is negligibly small at small superfluid velocities. In this sense, the superfluidity of 2D magnetoexcitons keeps to be almost metastable one. This can be shown by the estimation of the probability  $dW$  of the excitation of the quasiparticle on the plateau with magnetic momenta  $P \gg 1/r_B$ ; the energy of quasiparticles on the plateau  $\varepsilon(P)$  equals to the magnetoexciton binding energy.

At the motion of magnetoexciton liquid in a graphene lattice with the small velocity  $\mathbf{u}$ , which is smaller than the sound velocity  $c_s$ , according to the Landau criterion<sup>34</sup> creation of the quasiparticles in the region of plateau at great momenta with the magnetic momentum  $P \gg 1/r_B$  and the energy  $\sim E_b$  is possible due to the friction between liquid and impurities, defects in the lattice or roughness of boundaries of the graphene layers. So, when one quasiparticle appears the liquid gets the magnetic momentum  $P$ . The appearance of the large magnetic momentum in the liquid is equivalent to the great mean separation between electron and hole along one layer  $\rho = r_B^2 [\mathbf{B}, \mathbf{P}] / B$ . So, magnetoexcitons with *very* large  $P$  does not exist due to the interaction of electron and hole with impurities, etc.

Let us estimate the probability  $dW_P$  of the transition of the superfluid system from the initial state with the magnetic momentum  $P=0$  without quasiparticles to the final state with one quasiparticle with the large magnetic momentum  $P \gg 1/r_B$  by using Fermi golden rule by taking into account the ‘‘friction’’ interaction  $V_f$ . We have for the probability per unit time  $dW(P)$ ,

$$dW(P) = \frac{2\pi}{\hbar} |\langle 0 | \hat{V}_f \hat{\alpha}^\dagger | 0 \rangle|^2 \delta[\Delta E_k + \varepsilon(P) + \mathbf{P}\mathbf{u}] d\nu_\varepsilon, \quad (37)$$

where  $\nu_\varepsilon$  is the density of final states of the system,  $\Delta E_k$  is the change in the kinetic energy of superfluid liquid,  $\hat{V}$  is the

friction interaction,  $|0\rangle$  is a ground state of magnetoexciton superfluid, and  $\hat{\alpha}_\mathbf{p}^\dagger$  is the quasiparticle creation operator. After quasiparticle creation total magnetic momentum of the system is conserved.

At large momentum  $P \gg 1/r_B$ , the wave function of quasiparticle is almost the same as wave function of the isolated magnetoexciton. It means that the quasiparticle annihilation operator  $\hat{\alpha}_\mathbf{p}$  is almost the same as the ordinary particle annihilation operator  $a_\mathbf{p}$ .

In second quantified representation, the friction interaction operator  $\hat{V}$  can be represented as

$$\hat{V}_f = \sum_{\mathbf{p}'\mathbf{p}''} V_{f\mathbf{p}'\mathbf{p}''} \hat{\alpha}_{\mathbf{p}'}^\dagger a_{\mathbf{p}''}, \quad (38)$$

where  $V_{f\mathbf{p}'\mathbf{p}''}$  is the matrix element of friction interaction that is calculated with the use of isolated magnetoexciton eigenfunctions [Eq. (4)]. Due to the factor  $\exp[-r^2/(4r_B^2)]$  in Eq. (7)  $\langle 0 | \hat{V}_f \hat{\alpha}^\dagger | 0 \rangle \rightarrow 0$  at  $P \gg r_B$ . Thus, the probability  $dW_P$  of the creation of the quasiparticle with the large magnetic momenta  $P \gg 1/r_B$  is negligibly small. So, the superfluidity of 2D magnetoexcitons keeps to be almost metastable one. Note that at small magnetic momenta  $P \ll 1/r_B$  in the region of the sound spectrum of interacting magnetoexcitons Landau criterion of superfluidity is valid and the probability  $dW_P$  of the creation of the quasiparticle in the region of the sound spectrum at  $u < c_s$  is zero due to  $\delta[\Delta E + \varepsilon(P) + \mathbf{P}\mathbf{u}] = 0$  in Eq. (37).

At low temperatures  $T < T_c \ll E_b$ , states with large magnetic momenta are negligibly filled ( $\exp[-\varepsilon(P)/(k_B T)] \ll 1$ , where  $\varepsilon(P)$  is the magnetoexciton energy, which has the same order as magnetoexciton binding energy  $E_b$ ; at high magnetic fields  $E_b = 4\sqrt{\pi/2} e^2 / (\epsilon r_B)$  at  $D \ll a(B, D)$  and  $E_0 = 4e^2 / (\epsilon D)$  at  $D \gg a(B, D)$ ). So, quasiparticles at large magnetic momenta  $P$  give a small contribution to the densities of the normal component  $n_n$  and superfluid component  $n_s$  [see Eq. (33)]. Hence, the expressions given above for the temperature of Kosterlitz-Thouless transition are valid.

Note that the contributions to the single-electron Hamiltonian from the Zeeman splitting and very small pseudospin splitting (caused by two valleys in graphene) set identically to zero analogously to Ref. 29. We assume the energy degeneracy respect to two possible spin projections and two graphene valleys (two pseudospins) for an electron and a hole. The Zeeman term is much smaller than the characteristic separation between the nearest Landau levels. The ratio of the contribution to the energy from the Zeeman term  $\Delta E_Z(B)$  to the characteristic separation between the nearest Landau levels  $\Delta E_L(B)$  is negligible [at  $B=10T$ , this ratio is  $\Delta E_Z(B)/\Delta E_L(B) \approx \mu_B B / (\sqrt{2} \hbar v_F r_B^{-1}) \approx 5 \times 10^{-3}$ , where  $\mu_B = \hbar e / (2m_e c)$  is the Bohr magneton and  $m_e$  is the mass of a free electron]. Besides, the Zeeman term is negligible compare to the binding energy of a magnetoexciton on the lowest Landau level [at  $B=10 \text{ T}$  and  $D=2 \text{ nm}$  this ratio is  $\Delta E_Z(B)/E_b \approx 9 \times 10^{-4}$ ]. The Zeeman term is much smaller than the chemical potential  $\mu$  corresponding to the dipole-dipole repulsion between magnetoexcitons [at  $n=10^{10} \text{ cm}^{-2}$ ,  $B=10 \text{ T}$ , and  $D=2 \text{ nm}$ , this ratio is  $\Delta E_Z(B)/\mu \approx 10^{-2}$ ]. Therefore, the Zeeman term is negligible compare to all energies in this system.

## VI. DISCUSSION

The rare excitonic system is stable at  $D < D_{cr}(B)$  and  $T=0$  when the magnetoexciton energy  $E_{exc}(D, H)$  [given in Eq. (21)] is larger than the sum of activation energies  $E_L = ke^2/(\epsilon r_B)$  for incompressible Laughlin liquids of electrons or holes in the fractional quantum Hall effect regime in graphene;  $k=0.06$  for the filling factor  $\nu=1/3$  at the Landau level  $n_L=1$  and the number of particles  $N$  corresponding to  $N^{-1} \approx 0.16$ , etc.<sup>28</sup> For coupled quantum wells, the activation energy is for incompressible Laughlin liquids of electrons or holes at  $\nu=1/3$  at the Landau level  $n_L=0$  is the same as for graphene at the Landau level  $n_L=1$  (compare to Ref. 16). Since  $k \ll 1$ , the critical value  $D_{cr} \gg r_B$ . In this case, one has  $E_{exc} = 4e^2/(\epsilon D)(1 - 2r_B^2/D^2)$  for a magnetoexciton with quantum numbers  $n_+ = n_- = 1$ . Since in the dilute system in high magnetic fields  $\mu \ll E_{ex}$ , the contribution to the energy from the dipole-dipole repulsion between magnetoexcitons can be neglected compare to the binding energy of magnetoexciton. As a result, we have from the stability condition  $D_{cr} = 2^{-1/2} r_B (\sqrt{2/k} - k/\sqrt{2})$ . For greater  $\nu$ , it gives an upper bound on  $D_{cr}$ . The excitonic phase is more stable than the Laughlin states of electrons and holes at a given Landau filling  $\nu$  if  $D < D_{cr}$ . Below the Kosterlitz-Thouless temperature, one can observe the appearance of persistent currents in separate graphene layer. Note that in some region of Landau filling inside  $(0, \nu_{cr})$ , crystal phase of indirect magnetoexcitons must exist in bilayer graphene (analogous to Ref. 38).

The appearance of local superfluid density above  $T_c$  can be manifested, for example, in observations of temperature dependence of the exciton diffusion on intermediate distances (with the help of local measurements of exciton photoluminescence at two points using optical fibers or pinhole). The superfluid state at  $T < T_c$  can manifested itself in the existence of persistent (“superconducting”) oppositely directed electric currents in each graphene layer. The interlayer tunneling in an *equilibrium* spatially separated electron-hole system (our case 2) leads to interesting Josephson phenomena in the system: to a transverse Josephson current, inhomogeneous (many sin-Gordon soliton) longitudinal currents,<sup>6</sup> diamagnetism in a magnetic field  $\mathbf{B}$  parallel to the junction (when  $B$  is less than some critical value  $B_{c1}$ , depending on the tunneling coefficient), and a mixed state with

Josephson vortices for  $B > B_{c1}$  (in addition, taking tunneling into account leads to a loss of symmetry of the order parameter and to a change in the character of the phase transition). The interlayer resistance relating to the drag of electrons and holes can also be a sensitive indicator of the transition to the superfluid of the electron hole system.<sup>10</sup>

In conclusion, we have studied BEC and superfluidity of magnetoexcitons in two graphene layers with applied external voltage in perpendicular magnetic field. We have reduced the problem of exciton at  $B=0$  and in a renormalized random field depending on  $H$ . The superfluid density  $n_S(T)$  and the temperature of the Kosterlitz-Thouless phase transition to the superfluid state have been calculated. We have shown that at fixed exciton density  $n$ , the Kosterlitz-Thouless temperature  $T_c$  for the onset of superfluidity of magnetoexcitons decreases as a function of magnetic field like  $B^{-1/2}$  at  $D \lesssim r_B$  and as  $B^{-2}$  when  $D \gg r_B$ . We have shown that  $T_c$  increases when the density  $n$  increases and decreases when the magnetic field  $B$  and the interlayer separation increase. The advantage of the observation of magnetoexciton superfluidity and BEC in graphene in comparison with this in CQWs consists of essentially weak influence of the random field on  $T_c$  due to the fact that the density of defects in graphene is sufficiently lower than in CQWs (due to the absence of the roughness of QWs boundaries). Another thing which makes the observation of the 2D magnetoexcitonic BEC in two-layer graphene easier than in CQWs is the fact that the available effective mass of magnetoexciton in graphene can be essentially smaller than in CQWs because in the latter only in sufficiently strong magnetic fields manifests  $m_B \gg m_e + m_h$ , while in graphene,  $m_e = m_h = 0$ . Note that we considered the superfluidity in two cases: case 1, when electrons and holes are created by the gates and are in the equilibrium with each other, and case 2, when electrons and holes are created by the laser pumping and the magnetoexcitons are in quasiequilibrium thermodynamical state.

## ACKNOWLEDGMENTS

Y.E.L. was supported by grants from RFBR and INTAS. G.G. acknowledges partial support from Contract No. FA 9453-07-C-0207 of AFRL.

<sup>1</sup>D. W. Snoke, Science **298**, 1368 (2002).

<sup>2</sup>L. V. Butov, J. Phys.: Condens. Matter **16**, R1577 (2004).

<sup>3</sup>J. P. Eisenstein and A. H. MacDonald, Nature (London) **432**, 691 (2004).

<sup>4</sup>V. B. Timofeev and A. V. Gorbunov, J. Appl. Phys. **101**, 081708 (2007).

<sup>5</sup>Yu. E. Lozovik and V. I. Yudson, JETP Lett. **22**, 26 (1975); Sov. Phys. JETP **44**, 389 (1976); Yu. E. Lozovik and I. V. Ovchinnikov, Phys. Rev. B **66**, 075124 (2002).

<sup>6</sup>A. V. Klyuchnik and Yu. E. Lozovik, Sov. Phys. JETP **49**, 335 (1979); Yu. E. Lozovik and A. V. Poushnov, Phys. Lett. A **228**, 399 (1997).

<sup>7</sup>J. Zang, D. Schmeltzer, and J. L. Birman, Phys. Rev. Lett. **71**, 773 (1993).

<sup>8</sup>Xu Zhu, P. B. Littlewood, M. S. Hybertsen, and T. M. Rice, Phys. Rev. Lett. **74**, 1633 (1995).

<sup>9</sup>S. Conti, G. Vignale, and A. H. MacDonald, Phys. Rev. B **57**, R6846 (1998).

<sup>10</sup>G. Vignale and A. H. MacDonald, Phys. Rev. Lett. **76**, 2786 (1996).

<sup>11</sup>Yu. E. Lozovik and O. L. Berman, JETP Lett. **64**, 573 (1996); JETP **84**, 1027 (1997).

<sup>12</sup>Yu. E. Lozovik, O. L. Berman, and M. Willander, J. Phys.: Condens. Matter **14**, 12457 (2002).

- <sup>13</sup>I. V. Lerner and Yu. E. Lozovik, *Sov. Phys. JETP* **51**, 588 (1980).
- <sup>14</sup>D. Paquet, T. M. Rice, and K. Ueda, *Phys. Rev. B* **32**, 5208 (1985).
- <sup>15</sup>C. Kallin and B. I. Halperin, *Phys. Rev. B* **30**, 5655 (1984); **31**, 3635 (1985).
- <sup>16</sup>D. Yoshioka and A. H. MacDonald, *J. Phys. Soc. Jpn.* **59**, 4211 (1990).
- <sup>17</sup>Yu. E. Lozovik and A. M. Ruvinsky, *Phys. Lett. A* **227**, 271 (1997); *JETP* **85**, 979 (1997).
- <sup>18</sup>M. A. Olivares-Robles and S. E. Ulloa, *Phys. Rev. B* **64**, 115302 (2001).
- <sup>19</sup>S. A. Moskalenko, M. A. Liberman, D. W. Snoke, and V. V. Botan, *Phys. Rev. B* **66**, 245316 (2002).
- <sup>20</sup>K. S. Novoselov, A. K. Geim, S. V. Morozov, D. Jiang, Y. Zhang, S. V. Dubonos, I. V. Grigorieva, and A. A. Firsov, *Science* **306**, 666 (2004).
- <sup>21</sup>Y. Zhang, J. P. Small, M. E. S. Amori, and P. Kim, *Phys. Rev. Lett.* **94**, 176803 (2005).
- <sup>22</sup>D. P. DiVincenzo and E. J. Mele, *Phys. Rev. B* **29**, 1685 (1984); C. L. Kane and E. J. Mele, *Phys. Rev. Lett.* **78**, 1932 (1997).
- <sup>23</sup>S. Das Sarma, E. H. Hwang, and W.-K. Tse, *Phys. Rev. B* **75**, 121406(R) (2007).
- <sup>24</sup>K. S. Novoselov, A. K. Geim, S. V. Morozov, D. Jiang, M. I. Katsnelson, I. V. Grigorieva, S. V. Dubonos, and A. A. Firsov, *Nature (London)* **438**, 197 (2005).
- <sup>25</sup>Y. B. Zhang, Y.-W. Tan, H. L. Stormer, and P. Kim, *Nature (London)* **438**, 201 (2005).
- <sup>26</sup>Y. Zhang, Z. Jiang, J. P. Small, M. S. Purewal, Y.-W. Tan, M. Fazlollahi, J. D. Chudow, J. A. Jaszczak, H. L. Stormer, and P. Kim, *Phys. Rev. Lett.* **96**, 136806 (2006).
- <sup>27</sup>K. Nomura and A. H. MacDonald, *Phys. Rev. Lett.* **96**, 256602 (2006).
- <sup>28</sup>C. Töke, P. E. Lammert, V. H. Crespi, and J. K. Jain, *Phys. Rev. B* **74**, 235417 (2006).
- <sup>29</sup>A. Iyengar, Jianhui Wang, H. A. Fertig, and L. Brey, *Phys. Rev. B* **75**, 125430 (2007).
- <sup>30</sup>V. Lukose, R. Shankar, and G. Baskaran, *Phys. Rev. Lett.* **98**, 116802 (2007).
- <sup>31</sup>L. P. Gorkov and I. E. Dzyaloshinskii, *Sov. Phys. JETP* **26**, 449 (1967).
- <sup>32</sup>B. I. Halperin and T. M. Rice, *Solid State Phys.* **21**, 115 (1968).
- <sup>33</sup>L. V. Keldysh and A. N. Kozlov, *Sov. Phys. JETP* **27**, 521 (1968).
- <sup>34</sup>A. A. Abrikosov, L. P. Gorkov, and I. E. Dzyaloshinski, *Methods of Quantum Field Theory in Statistical Physics* (Prentice-Hall, Englewood Cliffs, NJ, 1963).
- <sup>35</sup>A. Griffin, *Excitations in a Bose-Condensed Liquid* (Cambridge University Press, Cambridge, England, 1993).
- <sup>36</sup>Yu. E. Lozovik and V. I. Yudson, *Physica A* **93**, 493 (1978).
- <sup>37</sup>J. M. Kosterlitz and D. J. Thouless, *J. Phys. C* **6**, 1181 (1973); D. R. Nelson and J. M. Kosterlitz, *Phys. Rev. Lett.* **39**, 1201 (1977).
- <sup>38</sup>X. M. Chen and J. J. Quinn, *Phys. Rev. Lett.* **67**, 895 (1991).